

## PRE-ASSESSMENT TOOL FOR DISTORTION IN FRAME-LIKE COMPOSITE STRUCTURES: INDUSTRIAL APPLICATION

Maximilian Lipcan<sup>1,2</sup>, Johannes Mattheus Balvers<sup>1</sup>

<sup>1</sup> Airbus Helicopters Deutschland GmbH, Industriestraße 4, 86609 Donauwörth, Germany  
Email: maximilian.lipcan@airbus.com, Web Page: <http://www.airbushelicopters.com/>

<sup>2</sup> Institute for Carbon Composites, Technische Universität München, Boltzmannstr. 15, 85748  
Garching, Germany, Web Page: <http://www.lcc.mw.tum.de/>

**Keywords:** distortion, manufacturing process simulation, early design

### Abstract

Especially in the aerospace industry, composites that are manufactured by, for instance, the autoclave process or resin transfer moulding need to meet high standards with respect to geometrical design tolerances. There are several drivers within the trinity of material, design and process that could result in a distorted part after manufacturing. The subsequent compensation of this distortion in the assembly is a costly and mostly a time-consuming process.

Currently, the (commercially) available simulation tools to predict distortion require extensive information about the material, design and process. Hence, they are mostly applied towards the end of the development stage of a product. In concurrent engineering, in which part design and tooling development are parallel operations, these simulations may deliver too late the output for implementing countermeasures in tooling design. It is therefore strived for a pre-assessment tool for the early design phase that identifies earlier composite parts prone to distortion. In the following, the necessary steps are shown to identify and determine analytically the needed cross-sectional parameters. With these parameters the distortion trend for a given frame structure can then be analysed.

### 1. Introduction

The overall aim of this study is to address the variation in dimensions based on the manufacturing at an early stage of the design of composites helicopter frames. To estimate the process-induced deformation (PID) of such structures without having to create a full-scale finite-element(FE) model, their geometrical description is coupled to the equations of spring-in due to the anisotropically thermoelastic and chemical shrinkage. Assuming that these two factors are amongst the main drivers of distortion during manufacturing [1], this method can present a fast way to predict tendencies without the need of detailed process or manufacturing data. Even during concurrent engineering, the timetable of the affected part can then be adapted to incorporate a detailed analysis to modify the tooling geometry.

It has been shown that the thermoelastic change in shape for simple curved composite laminates can be extended towards the curvature change of curved sandwich panels [2,3]. For an anisotropic material, whether it is a monolithic or a sandwich composite, the so-called “spring-in” can be predicted based on the initial geometry, the temperature change and the coefficient of thermal expansion in radial (through the thickness) and tangential direction. Additionally the non-thermoelastic cure shrinkage can be taken into account with an additional term [4]:

$$\Delta\theta = \theta \left\{ \left[ \frac{(\alpha_t - \alpha_r)\Delta T}{(1 + \alpha_r\Delta T)} \right] + \left[ \frac{(\phi_t - \phi_r)}{(1 + \phi_r)} \right] \right\} \quad (1)$$

where:

$\Theta$  = included angle

$\Delta\Theta$  = change in included angle

$\alpha_r$  = radial coefficient of thermal expansion

$\alpha_t$  = tangential coefficient of thermal expansion

$\Delta T$  = change in temperature

$\phi_t$  = tangential, isothermal shrinkage

$\phi_r$  = radial isothermal shrinkage

With the same assumptions as for sandwich panels, the spring-in behaviour of a simple I-section composite frame was investigated analytically [5]. In the following work a procedure is proposed to adapt and expand this idea to determine the distortion of arbitrary frame-like structures.

## 2. Modelling

### 2.1. Description of approach

It has been shown in literature [1,6,7] and from conducted case studies, that the strain anisotropy of thermal expansion and cure shrinkage is responsible for most of the manufacturing distortion during curing for thicker laminates ( $\geq 4\text{mm}$ ). Therefore if this effect is calculated in an analytical way by obtaining the different values of expansion along and normal to the curvatures at any given point of a spline representing a frame-like structure, the thermoelastic deformation behaviour of the complete part can be approximated. Based on an established method to homogenize sublaminates, the approach is extended towards a complete cross-section consisting of several such laminated walls. The area of two walls forming a t-joint is investigated in more detail since its local properties are strongly varying along its geometry. For a given frame-like structure, each local change of layup or geometry results in a new set of values. These values are then used with Equation 1 to retrieve a section-wise spring-in behaviour. By summation the deformation shape of the part is obtained driven by the former mentioned effect of strain mismatch.

### 2.2. Geometrical definition of the cross-sectional area

An arbitrary cross-section of a beam-like structure can be described as an assembly of several single flat walls [8]. Each wall has its own set of tangent ( $s_i$ ) and normal ( $n_i$ ) axes. The orientation of  $i$ -th wall is then given by the angle  $\gamma_i$  and the distance ( $\bar{y}_i, \bar{z}_i$ ) of its centre to the chosen origin (see Figure 1). The darker coloured wall at the centre of the T-joint represents a gusset filler location, which based on its geometry needs to be treated differently than the other laminated walls. So far it is assumed that the cross section remains constant and local spring-in effects are not included in the calculation of the global behaviour.

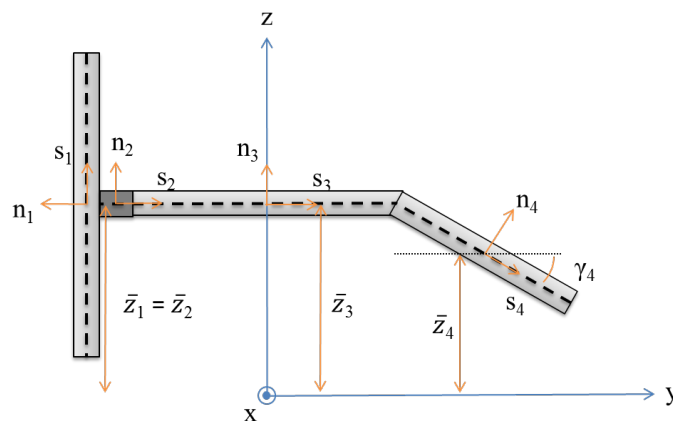


Figure 1. Cross section and reference system

### 2.3. Homogenization of the flat laminated walls

To derive the properties of each laminated wall, a method of volume averaging the stiffness for either constant stresses or strains is used [9]. For a homogenous stress or strain distribution within a single wall, where the x-direction is the principle direction and  $s_i$  and  $n_i$  the second respectively the third direction, the equilibrium and compatibility considerations require a continuity of the in-plane strains  $\varepsilon_{11}$ ,  $\varepsilon_{22}$ ,  $\varepsilon_{12}$  and the through-the thickness stresses  $\sigma_{33}$ ,  $\sigma_{23}$ ,  $\sigma_{13}$ . If the constant stresses and strains are grouped:

$$\sigma_{new} = T\sigma_{old} = [\langle\sigma_{33}\rangle \ \langle\sigma_{23}\rangle \ \langle\sigma_{13}\rangle \ \sigma_{11} \ \sigma_{22} \ \sigma_{12}] = \begin{Bmatrix} \langle\sigma_a\rangle \\ \sigma_b \end{Bmatrix} \quad (2)$$

Then the following reordered stiffness matrix is obtained for an arbitrary in-plane rotated orthotropic ply:

$$TCT^T = \begin{Bmatrix} C_{33} & 0 & 0 & C_{33} & C_{23} & C_{34} \\ 0 & C_{55} & C_{56} & 0 & 0 & 0 \\ 0 & C_{56} & C_{66} & 0 & 0 & 0 \\ C_{13} & 0 & 0 & C_{11} & C_{12} & C_{14} \\ C_{23} & 0 & 0 & C_{21} & C_{22} & C_{24} \\ C_{34} & 0 & 0 & C_{41} & C_{24} & C_{44} \end{Bmatrix} = \begin{Bmatrix} C_{aa} & C_{ab} \\ C_{ab}^T & C_{bb} \end{Bmatrix} \quad (3)$$

Separating the stress-strain equation whether the values are constant through the laminate, one obtains:

$$\begin{Bmatrix} \varepsilon_a \\ \sigma_b \end{Bmatrix} = \begin{Bmatrix} C_{aa}^{-1} & C_{aa}^{-1}C_{ab} \\ C_{ab}^T C_{aa}^{-1} & -C_{ab}^T C_{aa}^{-1}C_{ab} + C_{bb} \end{Bmatrix} \begin{Bmatrix} \langle\sigma_a\rangle \\ \langle\varepsilon_b\rangle \end{Bmatrix} \quad (4)$$

Subsequently volume averaging it and solving it, yields the following equation for the volume averaged stress:

$$\begin{Bmatrix} \langle\sigma_a\rangle \\ \langle\sigma_b\rangle \end{Bmatrix} = \underbrace{\begin{Bmatrix} A^{-1} & A^{-1}B \\ B^T A^{-1} & B^T A^{-1}B + D \end{Bmatrix}}_{C_{ij}} \begin{Bmatrix} \langle\varepsilon_a\rangle \\ \langle\varepsilon_b\rangle \end{Bmatrix} \quad (5)$$

with:

$$A = \langle C_{aa}^{-1} \rangle$$

$$B = \langle C_{aa}^{-1} C_{ab} \rangle \quad (6)$$

$$D = \langle -C_{ab}^T C_{aa}^{-1} C_{ab} + C_{bb} \rangle$$

where:

$\langle \cdot \rangle$  = term by term volume averaging

Once the re-ordering is reversed and the stresses and strains are in their initial order, the homogenized stiffness for the wall in its coordinate system is obtained:

$$\{\sigma\} = \underbrace{T^{-1} C_{ij} T^{-T}}_{\bar{C}_{ij}} \{\varepsilon\} \quad (7)$$

with

$\bar{C}_{ij}$  = homogenized stiffness matrix in initial (1, 2, 3)-system

To calculate the homogenized coefficients of thermal expansion  $|\alpha|$ , a similar procedure is used, which yields:

$$\begin{Bmatrix} \langle \alpha_a \rangle \\ \langle \alpha_b \rangle \end{Bmatrix} = \frac{1}{\Delta T} \begin{Bmatrix} -BD^{-1}F - E \\ D^{-1}F \end{Bmatrix} \quad (8)$$

With

$$E = \langle C_{aa}^{-1} (C_{aa}\alpha_a + C_{ab}\alpha_b)\Delta T \rangle \quad (9)$$

$$F = \langle C_{ab}^T C_{aa}^{-1} (C_{aa}\alpha_a + C_{ab}\alpha_b)\Delta T + (C_{ab}^T\alpha_a + C_{bb}\alpha_b)\Delta T \rangle$$

where:

$\langle \cdot \rangle$  = term by term volume averaging

### 2.4. Homogenization of a gusset filler area

If the walls of the frame form a T-joint, a gusset filler is used to preserve the joint structural integrity and increase the out-of-plane load transfer capability [10]. The deltoid geometry at the transition zone of the “web” into the “flange, the so-called “gusset filler” consists here of several layers of fabric, which are stacked and then cut to the triangular shape (see Figure 2). Therefore almost isotropic properties are obtained for the gusset filler with the previous introduced homogenization method.

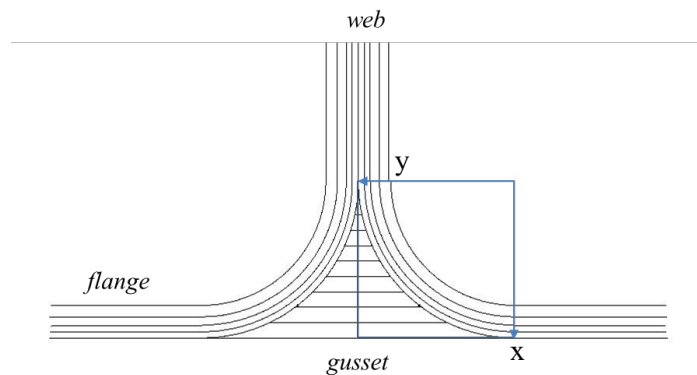


Figure 2. Gusset filler area of a T-joint

The radial shape of half the web ply and the underlying gusset filler (blue box in Figure 2) can be described by geometrical functions. The area of the ply is defined by two quarter circles, whereas the gusset area can be described as the subtraction of the circular area from a rectangular section. The radii of the two quarter circles are kept constant. It is assumed that the web plies are continuous without thickness changes.

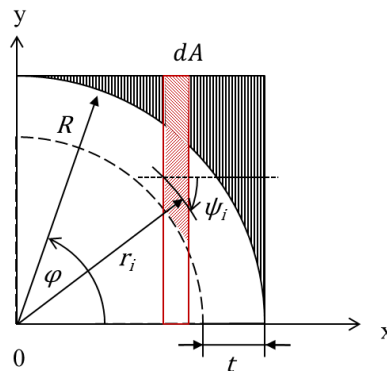


Figure 3. Shape function of the gusset filler and curved laminate

In case the gusset geometry is a square with its lateral length  $R$ , the area of each material can be calculated as follows:

$$A_{ply} = \int_0^R \sqrt{R^2 - x^2} dx - \int_0^{(R-t)} \sqrt{(R-t)^2 - x^2} dx \quad (10)$$

$$A_{gusset} = \int_0^R R - \sqrt{R^2 - x^2} dx \quad (11)$$

$$A_{total} = \int_0^R R - \sqrt{(R-t)^2 - x^2} dx \quad (12)$$

with

$R$  = radius of the web to flange transition

$t$  = laminate thickness

The area of an arbitrary partition  $dA$  can be calculated at any point in the interval  $[0, R]$ . For each material the area fraction within  $dA$  can be determined using either Equation 10 or 11 and by updating the integration interval accordingly. The angle of the laminate  $\psi$  changes along the radial direction. This means that the laminate angle varies along height at a given location  $x_0$ . An average between the lower and upper bound is used for calculation of the mechanical properties:

$$\psi(x) = \frac{1}{n} \sum_{i=1}^n \sin^{-1} \left( \frac{x}{r_i} \right) ; r_i = [(R-t), R] \quad (13)$$

Here the laminate thickness is kept constant along the complete radius. To include the case of radial ply drop-offs, which are commonly used in the industry, the thickness  $t$  would become an additional function of  $x$ .

To satisfy the compatibility requirement of equal in-plane strain and out-of-plane stress for the plies,  $dA$  is homogenized as displayed in Figure 3 with the third axis being the y-axis. The complete gusset area with ply and filler itself is homogenized with x-axis being the out-of-plane direction. The homogenized stiffness matrix of  $dA$  at any given location  $x$  is then:

$$\bar{C}_{ij}^{dA} = v_{dA ply}(x) T(\psi(x))^{-1} C_{ij}^{ply} T(\psi(x))^{-T} + v_{dA Gusset}(x) C_{ij}^{gusset} \quad (14)$$

$$ij = \{aa, ab, bb\}$$

where:

$$v_{dA i}(x) = \frac{dA_i}{dA} \quad (15)$$

With the described homogenization method in section 2.2 the three-dimensional mechanical properties of each partition  $dA$  can be calculated. In a subsequent step these properties are transferred to section coordinates of the web by rotating them with the given angle  $\gamma_{web} = \gamma_1$  (see Figure 4). Then again the properties are homogenized along the complete height of the gusset area with the volume fraction of each  $dA_i$ . As a result one set of properties for an arbitrary circular gusset filler area is retrieved.

## 2.5. Determination of the thermal expansion coefficients for the cross section

Based on the chosen cross-sectional Cartesian coordinate system (Figure 1) the corresponding values of expansion are calculated. To do so, the relevant ratio  $v_{x,y,z-i}$  of each wall for the given direction is

calculated and then used with Equations 8 and 9 for the averaging of the coefficient of thermal expansion over the complete cross-section.

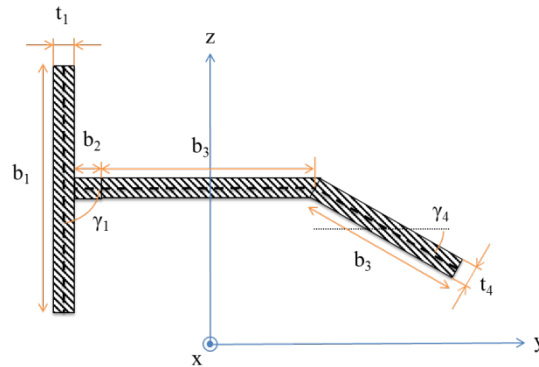


**Figure 4.** Dimensions of composite walls of a frame cross section

In the longitudinal direction the stresses are equally distributed over the complete area of the section and therefore:

$$v_{xi} = \frac{b_i t_i}{\sum_i^n b_i t_i} \quad (16)$$

For the in-plane properties of the section the ratio along the strain direction  $v_{z,y}$  of the complete section is calculated:

$$v_{zi} = \frac{b_i \sin \gamma_i + t_i \cos \gamma_i}{\left[ \max \left( \bar{z}_i + \frac{b_i}{2} \sin \gamma_i \right) - \min \left( \bar{z}_i - \frac{b_i}{2} \sin \gamma_i \right) \right]} \quad (17)$$

where:

$\bar{z}_i$  = distance of origin local coordinate-system ( $s_i, n_i$ ) to y-axis

Following these steps yields the analytically calculated resulting coefficients of expansion for each section in the desired tangential and normal direction.

## 2.6. Distortion analysis of a frame-like structure

In a first approximation, the spline geometry of a helicopter composite frame is described as a sum of  $k$  straight and radial sections. The total distortion in  $y$ -direction can then be expressed as the sum of each change in shape by using Equation 1:

$$\sum_{n=1}^k \left\{ \begin{array}{l} L_n \alpha_{l,n} \Delta T \sin \lambda_n ; f'' = 0 \text{ in } [x_{n-1}, x_n] \\ R_n \alpha_{r,n} \Delta T \sin \left( \Theta_n \left[ \frac{(\alpha_{t,n} - \alpha_{r,n}) \Delta T}{(1 - \alpha_{r,n} \Delta T)} \right] \right) ; f'' \neq 0 \text{ in } [x_{n-1}, x_n] \end{array} \right. \quad (18)$$

where:

$L_n$  = length of straight section

$R_n$  = radius of radial shape

$\Theta_n$  = enclosing angle of radial shape

$\lambda_n$  = origin angle of straight section

$\alpha_{r,n}$  = radial (through- the –thickness) coefficient of expansion  
 $\alpha_{t,n}$  = tangential coefficient of expansion (normal to cross section)

### 3. Application

In the following section, the proposed method is compared to the results of a phenomenological FE-simulation with the same set of ply properties. In the first step the method to determine the equivalent properties of the gusset area is tested. Then a complete section of a helicopter frame is investigated concerning its equivalent values of expansion in the different directions.

#### 3.1. Study I: Gusset filler

The used FE-Model of the T-joint with the gusset filler is shown in Figure 5. The transition of the web ply into the flange is modelled as a quarter circle with radius  $R = 10$  mm and a ply thickness of  $t = 2.12$  mm. The shrinkage effect of the epoxy resin is combined with the coefficient of thermal expansion into a so-called “enhanced CTE”. For the used epoxy material system the initial CTE of  $55 \cdot 10^{-6} \text{ K}^{-1}$  [11] increases then to  $78 \cdot 10^{-6} \text{ K}^{-1}$ [5]. The layup of the web-laminate consists of quasi-isotropically orientated prepreg fabric  $[(0/90)_n(\pm 45)_n]_s$ , whereas the layup of the flange contains additional UD –plies in x-direction. The gusset filler is made from stacked  $(\pm 45)_n$  fabric plies.

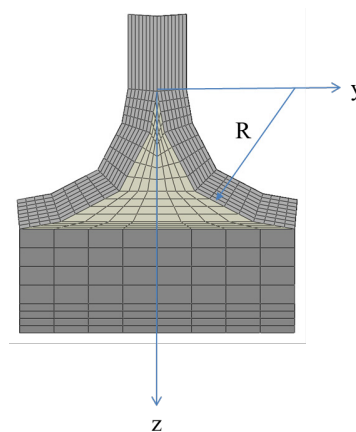


**Figure 5.** FE mesh of investigated gusset area

For an applied temperature difference of  $\Delta T = 160\text{K}$  the overall coefficients of expansion can be calculated from the nodal displacement. In the FE-simulation the in-plane coefficients in y-direction (Figure 6 left) are retrieved from the displacement of the exterior nodes located on the same height (Z-coordinate). The through-thickness CTE is calculated with the strain in z-direction between two adjacent nodes. In Figure 6 on the right side, the  $\text{CTE}_z$  between nodes is plotted with each set of coloured points representing the values of one row of nodes starting at  $z = 0$ . Additionally the black line displays the maximum value of each row. At  $z = 7.3$  mm there is a discontinuity which is related to the sharp edge between adjacent elements located in the middle of the quarter circle. The  $\text{CTE}_y$  starts at the value of the initial through-the-thickness CTE of the web-laminate and ends at its in-plane value, whereas in-between it is a mixture of the off-axis value of the web and the gusset filler. For the  $\text{CTE}_z$  the curve progression is vice versa starting at the in-plane value and converging towards the out-of-plane value of the web-laminate.

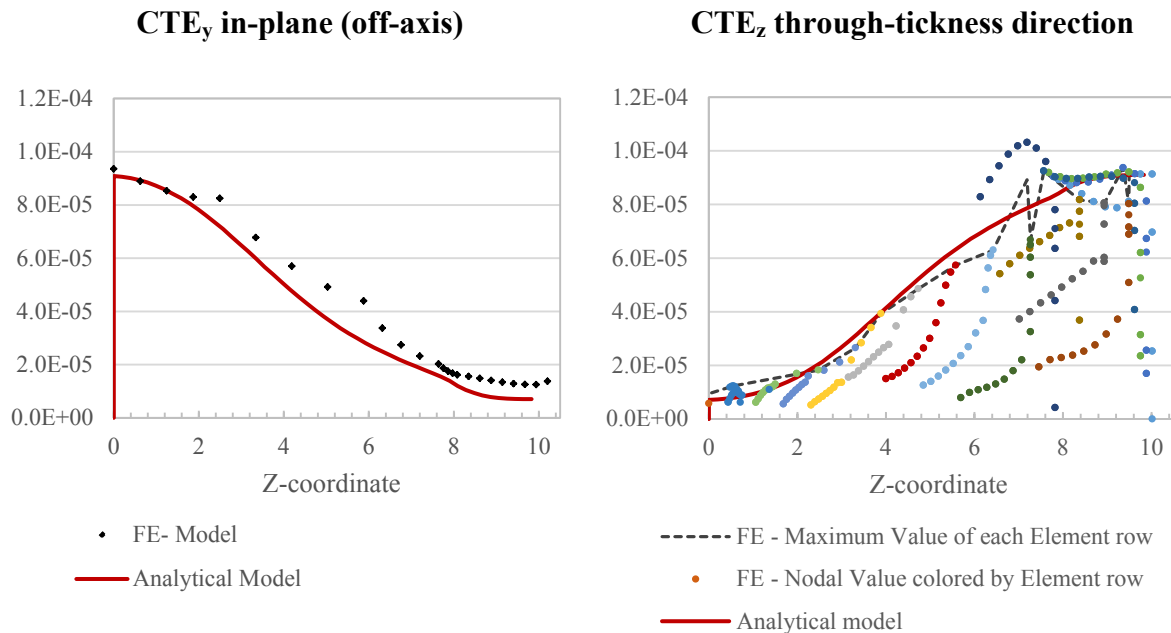


**Figure 6.** Comparison between FE and analytical coefficients of expansion in y- and z-direction

For the analytical approach, a python [12,13] script was developed, which calculates the stepwise area of the gusset and homogenizes the properties of the web laminate and the gusset filler. The solution fits the trend in both cases. The curve and value of the CTE<sub>y</sub> of the FE solution are met with a small deviation of the in-plane value at the end. The analytical approach matches more or less the maximum the through-the thickness direction CTE<sub>z</sub> value of the FE solution located near the centre of the gusset. This would nevertheless be the values of interest, since this area in the centre of the gusset represents the load carrying interface in z-direction between the flange and the web.

### 3.2. Study II: Sample section of a helicopter frame

With a suitable approximation of the expansion characteristics of the gusset area at the base of a t-section, a complete cross-section is now analysed. The section has a height of about 275 mm and a flanges width of 70 (lower) respectively 65 mm (upper flange). In this case the angle between the web and the flanges is 85°. Once again the web laminate is quasi-isotropic, whereas the flanges have additional layers of unidirectional reinforcement. The lower flange has double the amount of fabric plies and several additional UD plies in comparison to the upper flange. As it can be seen in Figure 7 on the left side, the gusset filler areas are located on both sides of the I-beam, where the web migrates into the flanges. The enclosing radius differs hereby (lower radius: 8.2 mm; upper radius: 7.8mm). The same material system and temperature range is used as in the previous paragraph. The results of a phenomenological simulation with ABAQUS are again compared with the analytical values of the thermal expansion. The simulation was performed with a FE solid mesh of the extruded cross section (depth 200 mm) as depicted in Figure 7 on the right-hand side.



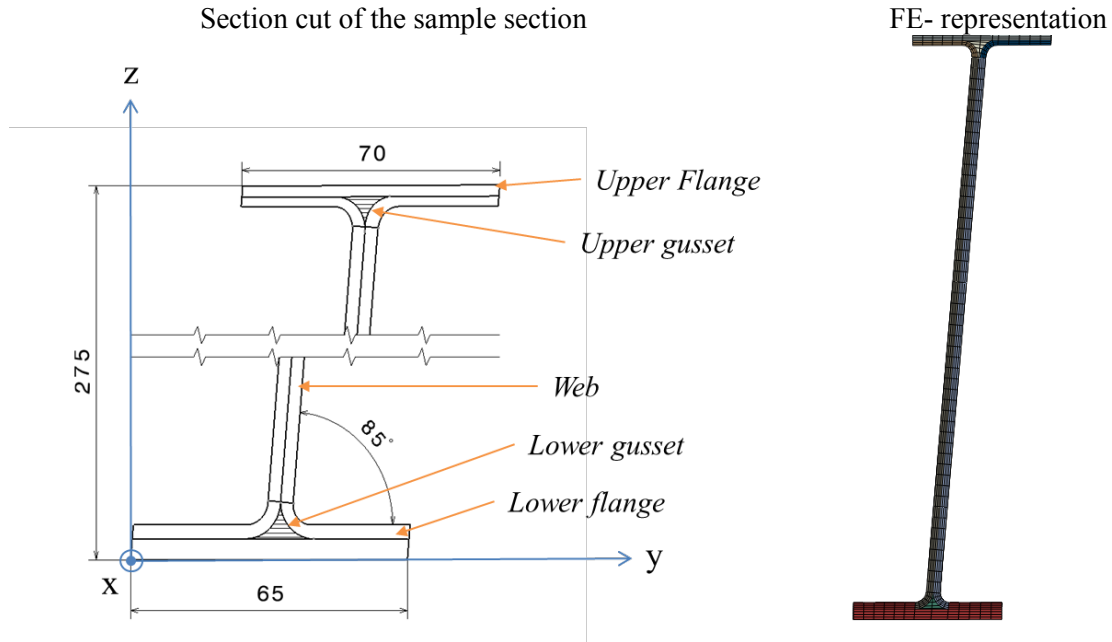


**Figure 7.** Dimensions of a sample cross section of a helicopter frame

For the analytical model, the frame was separated into the single members as depicted on the left-hand side of Figure 7. Additionally the lower gusset filler which encloses an angle of  $95^\circ$  needed to be split into two elements of  $90^\circ$  and  $5^\circ$  angle, since Equation 10-12 only work up until an enclosing angle of  $90^\circ$ . Furthermore this small wedge ensures to have a matching angle of the laminate  $\psi$  at all interfaces. The detailed separation of the gusset area for the analytical approach can be seen in Figure 8. To have a defined separation between the flange and the gusset, the lower area of the gusset which has similar properties as the flange laminate was still accounted as flange area. Therefore the homogenization of the gusset started at the flange surface (green box in Figure 8 starts at the upper edge of the flange instead of the gusset lower edge).

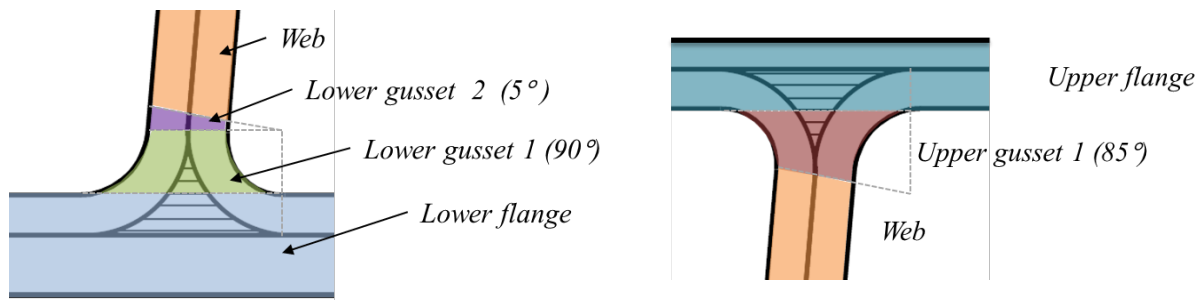


**Figure 8.** Separation of section for analytical homogenization

For the upper gusset only one element is needed since the enclosing angle is only  $85^\circ$ . In total, the properties of six elements were calculated separately. With the proposed method the “enhanced” coefficients in the x, y and z direction are determined. As shown in Figure 9, there are some differences visible in the coefficient of the single cross-sectional elements, but the overall “enhanced” thermal expansion, especially in the Z-direction matches rather well. The observed difference of the single elements comes from treating these separately, i.e. they can expand freely, in the analytical method. Only afterwards, they become constrained by their neighbouring elements. In the FE simulation, the expansion is determined from the “assembled” state.

Excerpt from ISBN 978-3-00-053387-7

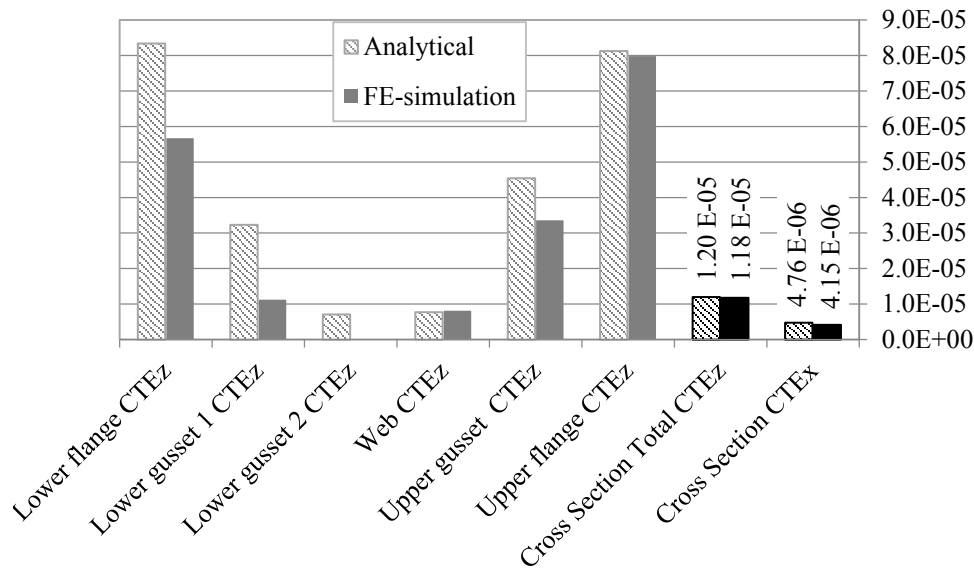


**Figure 9.** Calculated through the thickness CTE<sub>z</sub>'s and the longitudinal CTE<sub>x</sub> of the FE and analytical solution

#### 4. Conclusion and further work

A method is presented to estimate the global spring-in of frame-like structures. First it is outlined how a frame of a helicopter can be approximated with a central spline and varying cross-sections. In the next step it is shown how the geometry of an arbitrary cross section can be separated into single elements consisting of composite walls and gusset filler areas. Then a calculation method of homogenized 3D properties for the walls is summarized. To be able to equivalence the gusset area, a geometrical function is derived to determine the area fraction of the different materials at any given location. With the calculated properties and area fraction along the height of the gusset filler area, the homogenization method is used once again to obtain one set of 3D properties. With this approach it is possible to determine the coefficient of expansion in the desired directions of any frame section. The results of the method are subsequently compared to quasi-static phenomenological FE calculations. First the expansion of the gusset filler area including the web laminate and a circular gusset filler is investigated. Afterwards the results of complete section of a helicopter frame are compared. The proposed method shows good results compared to the state-of-the-art method widely used in the industry.

The next step would be to use the calculated data of all sections along a spline to estimate the frame deformation. The method possesses a great potential of performing each presented step as a part of an automated routine. An interface to the CAD environment or reading neutral data formats would even increase the applicability of this method. The effort of performing an assessment of the manufacturing distortion due to thermal strain mismatch and chemical shrinkage is then very low.

Still it has to be acknowledged that this method only provides an indication of deformation based on only two of the main drivers. Furthermore, no interaction between the in-plane spring-in effects of the cross-section and the global deformation is taken into account yet.

#### Acknowledgments

This study was performed in the framework of the project "MAI-TAI" funded by the German Federal Ministry for Education and Research (BMBF).

## References

- [1] J.M. Svanberg. Predictions of manufacturing induced shape distortions. Lulea University of Technology, 2002.
- [2] Y. Mahadik and K. Potter. Experimental investigation into the thermoelastic spring-in of curved sandwich panels. *Composites: Part A*, 49:68–80, 2013
- [3] G. Fernlund. Spring-in of angled sandwich panels. *Composites Science and Technology*, 65:317–323, 2005
- [4] D.W. Radford and T.S. Rennick. Separating Sources of Manufacturing Distortion in Laminated Composites. *Journal of Reinforced Plastics and Composites*, 19:621-641, 2000
- [5] M. Hartmann. Simple Methods for Strain Anisotropy Evaluation on a Generic I-Profile Frame Structure. *Proceedings of the Symposium on the occasion of the 5<sup>th</sup> anniversary of the Institute for Carbon Composites*, Munich, Germany, September 11th - 12th 2014
- [6] N. Ersoy, T. Garstka, K. Potter, M. R Wisnom, D. Porter, G. Stringer. Modelling of the spring-in phenomenon in curved parts made of a thermosetting composite. *Composites: Part A*, 41:410–418, 2010
- [7] C. Albert and G. Fernlund. Spring-in and warpage of angled composite laminates. *Composites Science and Technology*, 62:1895–1912, 2002
- [8] E. J. Barbero, R. Lopez-Anido, and J. F. Davalos. On the Mechanics of Thin-Walled Laminated Composite Beams. *Journal of Composite Materials*, 27: 806-829, 1993
- [9] J. Whitcomb and J. Noh. Concise Derivation of Formulas for 3D Sublaminar Homogenization. *Journal of Composite Materials*, 34: 522-535, 2000
- [10] J. W. Gillerspie Jr. and R. B. Pipes. Behaviour of Integral Composite Joints-Finite Element and Experimental Evaluation. *Journal of Composite Materials*, 12:408-421, 1978
- [11] Technical Data Sheet HexPly M18. Hexcel, 2007
- [12] G. Rossum. Python Reference Manual. *Technical Report*, CWI, Amsterdam, The Netherlands, 1995
- [13] S. van der Walt, S. C. Colbert and Gaël Varoquaux. The NumPy Array: A Structure for Efficient Numerical Computation. *Computing in Science & Engineering*, 13. 22-30, 2011